Design of super twisting disturbance observer-based controller for magnetic levitation system

A. M. Dongardive[1] · H. R. Mane[1] · R. H. Chile[1] · S. T. Hamde[1]

Abstract

The magnetic levitation systems are mismatched systems with inherent unstable nonlinear dynamics. This work has examined a control strategy that control and stabilize the magnetic levitation system from difficult start-up circumstances to the desired operating points in presence of uncertainties and disturbances. A cascaded super twisting disturbance observer (STDO)-based sliding mode controller is devised for both the electrical and electromechanical loops of the system. The overall stability of the system has been established. The performance of suggested control scheme is evaluated using simulation and experimentation. The performance of the suggested controller is compared with a classic proportional integral and derivative (PID) controller and a state and disturbance observer (SDO)-based controller. Performance criteria used for comparison are Integrated Squared Error(ISE), Integrated Absolute Error(IAE) and Time Weighted Absolute Error(ITAE). The suggested super twisting disturbance observer-based control scheme outperforms the other two and is able to control and stabilize magnetic levitation system in presence of parametric uncertainties and disturbances with smooth control.

1 Introduction

Magnetic **Lev**itation (Maglev) systems employ electromagnetic force to keep ferromagnetic items in the proper position in the air. An electromagnetic field created by maglev systems provides the electromagnetic force necessary for this technology. As a result of this capability, friction is removed, and material wear is decreased. Ground transportation has profited greatly from maglev systems, which may be used as active suspension systems [1,2]. They were regarded and used as the basic foundation for the development of mag-

netic train technology [3,4]. Maglev systems may be used in a variety of applications, including vibration isolation in sensitive equipment and high precision chip plate placement in photo-lithography [5] . When the system model is linearized in a small region, linear controllers are adequate, but they do not account for nonlinearities in the real system model. In contrast, nonlinear controllers regulate the system's dynamics globally rather than locally, allowing for real-time control. The search for a good topology for developing optimum nonlinear controllers will never stop, and the best one will meet the desired performance in a timely and promising manner. When choosing a nonlinear controller, the most important thing to evaluate is whether it provides a quick and efficient dynamic response, such as a short rising time, a short settling time, a decreased peak value, a low overshoot or undershoot, and a small steady-state error. Because real-world systems are subject to model uncertainty and external shocks, steady-state error is a possibility [6]. The nonlinear controller should be dealt with as smoothly and effectively as feasible. The bulk of nonlinear controllers perform poorly or not at all in the presence of uncertainty and disturbances. As a result, the primary goal of this study is to create a robust nonlinear controller for controlling the maglev system that can effectively

✉ A. M. Dongardive
1005arun@gmail.com

H. R. Mane
hmane43@gmail.com

R. H. Chile
rhchile@sggs.ac.in

S. T. Hamde
sthmade@sggs.ac.in

[1] Department of Instrumentation Engineering, S.G.G.S. Institute of Engineering and Technology, Nanded, Maharashtra, India

deal with uncertainties and disturbances while maintaining optimal dynamic behavior.

The design of control systems for Magnetic levitation and magnetic levitation-based systems is a well established and much addressed topic in the literature. An integral type control was built in [7], for bringing the magnetic bearing systems rotor to desired point and maintaining it at the appropriate location. The regulation of the maglev system was the subject of a comparative control analysis published in [8]. Experiments were carried out in order to compare the sliding mode controller (SMC) with a conventional controller. Further SMC strategies for the control of maglev and the systems based on maglev were presented in [9] and [10]. The employment of SMCs [9], static and dynamic type, ensured that the maglev system was controlled asymptotically while dealing with friction force and other unknowns. Intelligent SMC based on a radial basis function (RBF) network in [10] provides position tracking for the maglev system. Experiments in [11] demonstrated the performance of nonlinear adaptive and robust controllers on the regulation of the maglev system. In [12] a self-tuning stabilizing adaptive controller is proposed for the control of the repelling maglev system. In the mentioned investigation, the developed controller offered overall system stability and regulating precision without requiring a precise understanding of numerous components. Walter Barie and John Chiasson discuss how to construct and test nonlinear and linear state space controllers using velocity observers in [13]. The control systems used in the study were both based on linearized system models. The maglev system's location tracking problem was solved utilizing a resilient nonlinear control architecture by Yang et al. [14]. Physical parameter uncertainties, as well as modeling mistakes generated by these uncertainties, were accounted for in the control design, and the controller was built to tolerate them. The maglev system was controlled with proportional integral derivative (PID) type SMC controller as well as PID type dynamic SMC controllers in [15] . Another PID control solution to deal with the imbalanced vibration difficulties of an active magnetic bearing system was provided in [16]. To improve its efficiency, the described PID controller included a fuzzy gain tuning mechanism. Over the previous ten years, this issue has remained popular. The work presented in [17], mentioned the design of a PID controller enhanced with a velocity observer and a nonlinear feed forward technique to increase control quality and motion stability of a laboratory maglev system. A mix of linear quadratic Gaussian control, fault-tolerant control and multi-objective optimization were used to control an electromagnetic suspension system in [18]. In [19], a PID control based on real-time particle swarm optimization (PSO) was used to provide stability, balance, and propulsive placement for a maglev transit system. As suggested by Lin et al. in [20], another control method combination is made feasible using the PSO and

the PID. An adaptive PID controller is integrated with a PSO approach in this study to give the best learning rates for the adaptation rule, which work assured maglev system position monitoring. An adaptive control approach for the maglev system regulation was presented in [21], based on an online algebraic estimate of system parameters, linearization, and extended proportional-integral control. In [22], position tracking for a maglev suspension system was implemented using a nonlinear disturbance observer-based design of a robust nonlinear controller, whereas exponential tracking control of the maglev system was described in [23]. In [24], based on the back-stepping approach, a cognitive online auto-tune algorithm, a unique position tracking control algorithm, for a maglev system was developed. During the previous decade, the SMC technique has remained popular for controlling maglev systems.

Two of the different SMC examples of maglev control systems that can be found in the literature are the cascade structured SMC designs given in [5] and [25]. One more cascaded SMC approach based on two time-scale observer is proposed in [26]. Fractional order PID to ensure maglev system control is designed in [27]. In the aforementioned work, to accomplish fractional order PID control, model reference adaptive control was used in a closed-loop state and PID included a disturbance rejection mechanism. According to Uroš Sadek et al. [28], an upgraded adaptive fuzzy back-stepping controller was created for controlling the maglev system even in presence of uncertainty including parametric and structural. To regulate maglev systems, Baris Bidikli and Alper Bayrak [29] created and utilized a self-tuning robust integral of signum of error (RISE)-based controller in a cascade control system. The electromagnetic levitation system was controlled with a robust control architecture based on approximate feedback linearization in [30]. In [31], Fatih Adıgüzel et al. proposed an adaptive back-stepping control solution aimed to compensate for an iron ball's inaccuracy in position monitoring in a maglev system. To obtain a high-performance step response of the maglev system, Deepti Khimani et al. [32] built a nonlinear state feedback controller architecture. Humaidi in [33] proposed controllers for magnetic levitation systems based on linear and nonlinear active disturbance rejection. For magnetic suspension control of a low-speed maglev train, Yougang Sun et al. [34] developed a PID controller and an adaptive neural fuzzy SMC. For maglev system control, Sun et al. [35] has proposed SMC based on an exponential reaching law with RBF neural network estimator. For the nonlinear suspension system of maglev vehicles, Chen et al. [36] presented a unique RBF network approximation-based sliding mode adaptive controller architecture. When the popularity of the issue is taken into account, these examples may readily be broadened. The inspiration for this work came from a rigorous examination and evaluation of several controllers for the control of

MagLev systems that were given in the literature. Issues in the controllers that are now in use are dissected and studied and solutions to these challenges are suggested. In order to construct an uncertainty and disturbance compensation approach that decreases the trade-off between performance and stability while boosting robustness, SMC is the most extensively used in the literature to handle the control issues of Maglev. While going through all these controllers mentioned in the literature, one can understand that SMC-based controllers are able to tackle uncertainties and external disturbances. The well-known problem of SMC is chattering which is not suitable for such applications. Many techniques are mentioned in the literature to address the issue of chattering. A super twisting algorithm(STA) has been identified as one of the most powerful second-order continuous SMCs to tackle the same [37]. It was first published in [38], and it has since been used in a number of applications [39]. STA is a second-order sliding mode controller that can be used to control any generalized system using first-order sliding variable control. It has the advantage of just requiring information about the output sliding variable. It allows for and simultaneously gives convergence to the origin in a short amount of time. STA gives a smoother control effort due to the reduced chattering [40]. To make use of STA's smoothing capabilities, this work employs STA as an uncertainty and disturbance observer [41] and SMC as the primary controller.

The following are the primary contributions of the work.

1. The performance of a robust cascaded super twisting disturbance observer based SMC control technique is validated for model uncertainties and disturbance.
2. The developed control technique is used for maglev position control, and it perfectly matches the required trajectory with quicker convergence.
3. The use of the super twisting principle generates chattering free, smooth and continuous signal.
4. On the basis of the time-domain performance criteria , the results of STDO-based SMC controller are compared with SDO-based SMC and traditional PID controllers. STDO-based controller outperforms the others.
5. Extensive quantitative simulation and hardware experiments are used to prove the efficacy of the suggested method.

The robust control strategy has certainly been widely used for the control of a wide range of systems to cope with uncertainty, parametric and structural both, which are important issues in maglev system management. The input voltage is utilized to create the required electromagnet current in the electrical subsystem, which is then used to move the ferromagnetic material to the appropriate location. The required electromagnet current is first determined by STA-based uncertainty and disturbance observer-based controller
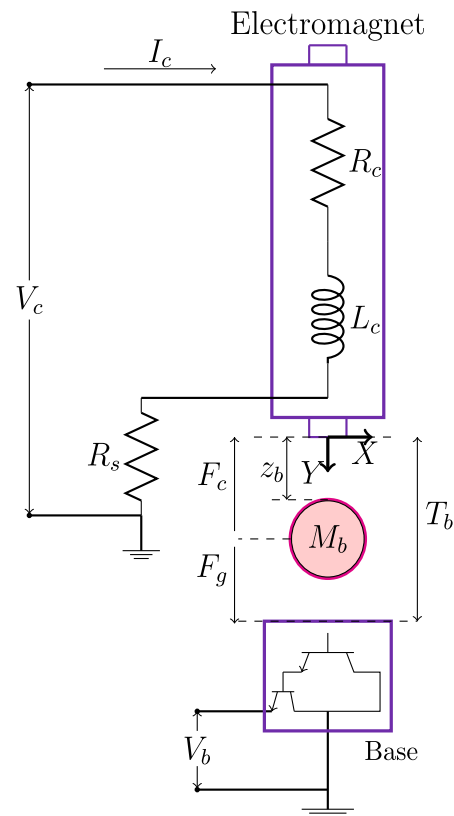

Fig. 1 Magnetic Levitation System Circuit Diagram

designed for the electromechanical subsystems and then the current value so determined is obtained from the electrical subsystem via similar type of controller.

The remainder of the paper is organized as follows: The basic idea of Maglev systems is outlined in Sect. 2, along with critical parameters and mathematical modeling. The STA-based uncertainty and disturbance observer-based controller design and architecture is discussed Sect. 3. The simulation results for the designed controller are a explained in this section as well. In Sect. 4 the conventional PID controller and state and disturbance observer-based controller are explained in brief and simulation results along with performance analysis of all three methods is given and explained. Experimental validation is given in 5 followed by discussion and comparison of results and the conclusion in Sect. 6

2 The magnetic levitation system: mathematical modeling

Figure 1 shows a circuit diagram for the Maglev system. A magnetic force is generated by a ferromagnetic coil, which lifts a steel ball into the correct position in the system. The placement of the ball is determined by the current flowing through the ferromagnetic coil and a sensor positioned at

the base position. The Maglev system is comprised of two subsystems, one of them is an electrical system and another electromechanical system.

2.1 Electrical system

When a voltage of V_c is applied to a ferromagnetic coil, as shown in Fig. 1, an electromagnetic field is formed. If Kirchhoff's voltage law is used for electrical loop the formula for V_c is obtained as:

$$\frac{1}{L_c}V_c = \frac{dI_c}{dt} + \frac{(R_c + R_s)}{L_c}I_c \tag{1}$$

The coil inductance is L_c, the coil current is I_c, and the coil resistance and current sensor resistance are R_c and R_s, respectively.

2.2 Electro mechanical system

The coil produces an electromagnetic field that acts on the ball, as denoted by the symbol F_c given by

$$F_c = \frac{K_m I_c^2}{2z_b^2} \tag{2}$$

The electromagnetic force constant is K_m, and the air gap between the ball and the electromagnet's face is $z_b > 0$. The gravitational attraction F_g exerted on the ball in the opposite direction is written as

$$F_g = M_b g \tag{3}$$

where the mass of the ball is represented by M_b and g represents gravitational acceleration. The ball's equation of motion can be written as,

$$\frac{d^2 z_b}{dt^2} = -\frac{K_m I_c^2}{2M_b z_b^2} + g \tag{4}$$

In state space, the Maglev system is represented as

$$\left.\begin{aligned} \dot{z}_1 &= z_2 \\ \dot{z}_2 &= -\frac{K_m z_3^2}{2M_b z_1^2} + g \\ \dot{z}_3 &= -\frac{(R_c + R_s)}{L_c}z_3 + \frac{1}{L_c}u \end{aligned}\right\} \tag{5}$$

which is obtained by placing, $z_1 = z_b$, $z_2 = \dot{z}_b$, $z_3 = I_c$ and $u = V_c$.

The main role of the controller is to control the position of the ball and make it follow the reference trajectory r. As indicated in the state space model, the dynamics of the

system includes L_c, R_s, g, M_b, R_c, and K_m, which are all unknown parameters. Furthermore, the system is not matched because the dynamics of z_2 are uncontrollable. To address the aforementioned challenges, the next section introduces a new approach of super twisting uncertainty and disturbance observer-based control for electromechanical as well as electrical subsystems.

3 Controller Design

A maglev system control is split into two components. In the first, the specified controller is used to obtain the electromagnet current for the electromechanical subsystem. This current is then utilized to regulate the electrical subsystem as a reference input.

As previously said, it is a mismatched system and in order to address the issue of uncertainty in the mismatched system, a virtual control input z_{3d} is developed, and a super twisting observer-based control is designed such that z_3 will follow z_{3d}. Defining the errors $e_1 = z_1 - r$, $e_2 = z_2 - \dot{r}$ and $e_3 = z_3 - z_{3d}$. In the error states form, the model in (5) may be expressed as

$$\dot{e}_1 = e_2 \tag{6}$$
$$\dot{e}_2 = -a_1 e_1 - a_2 e_2 + z_{3d} + \delta_1 \tag{7}$$
$$\dot{e}_3 = -a_3 z_3 + bu + \delta_2 \tag{8}$$

where a_1, a_2 and a_3 are nonzero constants and δ_1 and δ_2 are the disturbances expressed as

$$\delta_1 = a_1 e_1 + a_2 e_2 - \frac{K_m z_3^2}{2M_b z_1^2} + g - z_{3d} - \ddot{r} \tag{9}$$

$$\delta_2 = a_3 z_3 - bu - \frac{(R_s + R_c)}{L_c}z_3 + \frac{1}{L_c}u - z_{3d} \tag{10}$$

3.1 Super twisting disturbance observer-based controller design for electro mechanical system

In order to track the desired trajectory, being mismatched system, the virtual control input z_{3d} is obtained by using super twisting disturbance observer-based control. In compact form, the dynamics of e_1 and e_2 may be represented as:

$$\left.\begin{aligned} \dot{e} &= Ae + Bv + B\delta_1 \\ y &= Ce \end{aligned}\right\} \tag{11}$$

where $v = z_{3d}$, A, B, and C are matrices and are represented as,

$$A = \begin{bmatrix} 0 & 1 \\ -a_1 & -a_2 \end{bmatrix}; B = \begin{bmatrix} 0 \\ 1 \end{bmatrix}; C = \begin{bmatrix} 1 & 0 \end{bmatrix};$$

Where the vector e is : $e = \begin{bmatrix} e_1 & e_2 \end{bmatrix}^T$.

Defining sliding surface for this as ,

$$\sigma_1 = Ge \tag{12}$$

where $G = \begin{bmatrix} c_1 & 1 \end{bmatrix}$ and the constant c_1 is positive. When you differentiate (12) and use (11), you get (13) as

$$\dot{\sigma}_1 = GAe + GBv + GB\delta_1 \tag{13}$$

Design v as, $v = v_{eq} + v_n$. Where v_{eq} is designed such that it will compensate known terms as

$$v_{eq} = -(GB)^{-1}(GAe + k_1\sigma_1) \tag{14}$$

where k_1 is positive constant. Substituting (14) in (13) and solving (13) and v_n is designed to compensate unknown terms

$$v_n = -\hat{\delta}_1 \tag{15}$$

The estimate $\hat{\delta}_1$ is obtained as

$$\hat{\delta}_1 = k_2|\sigma_1|^{1/2} + v_1 \tag{16}$$
$$\dot{v}_1 = k_3 sat(\sigma_1) + \dot{\delta}_1 \tag{17}$$
$$\dot{\sigma}_1 = -k_1\sigma_1 + GB\tilde{\delta}_1 \tag{18}$$

where $\tilde{\delta}_1 = \delta_1 - \hat{\delta}_1$ represents an uncertainty estimation error.

Where k_1, k_2, k_3 are selected as positive constants. The function $sat(\sigma_1)$ is given as,

$$sat(\sigma_1) = \begin{cases} sign(\sigma_1) & \text{if } |\sigma_1| > \epsilon_1 \\ \frac{\sigma_1}{\epsilon_1} & \text{if } |\sigma_1| < \epsilon_1 \end{cases}$$

where ϵ_1 is a small positive constant.

3.2 Controller for the electrical subsystem

In order to achieve the objective of forcing $z_3 = z_{3d}$, a new approach of Super twisting disturbance observer-based control is proposed and explained in this section. Let us define another sliding surface as

$$\sigma_2 = e_3 \tag{19}$$

after differentiating (19) and using (8)

$$\dot{\sigma}_2 = -a_3 z_3 + bu + \delta_2 \tag{20}$$

u. is designed as $u = u_k + u_n$. Where u_k is intended to compensate for known terms as,

$$u_k = -\frac{1}{b}(-a_3 z_3 + k_4\sigma_2) \tag{21}$$

and u_n is designed for unknown terms as

$$u_n = -\frac{\hat{\delta}_2}{b} \tag{22}$$

The estimate $\hat{\delta}_2$ is obtained as

$$\hat{\delta}_2 = k_5|\sigma_2|^{1/2} + v_2 \tag{23}$$
$$\dot{v}_2 = k_6 sat(\sigma_2) + \dot{\delta}_2 \tag{24}$$
$$\dot{\sigma}_2 = -k_4\sigma_2 + \tilde{\delta}_2 \tag{25}$$

where k_4, k_5, k_6 are the positive constants and

$$\tilde{\delta}_2 = \delta_1 - \hat{\delta}_1 \tag{26}$$

function $sat(\sigma_2)$ is defined as,

$$sat(\sigma_2) = \begin{cases} sign(\sigma_2) & \text{if } |\sigma_2| > \epsilon_2 \\ \frac{\sigma_2}{\epsilon_2} & \text{if } |\sigma_2| < \epsilon_2 \end{cases}$$

where ϵ_2 is a small positive constant. The block diagram representing the proposed controller is shown in Fig. 2

3.3 The controller's stability analysis

In this section the stability of the proposed controller, is analyzed as stated in [6]. From the proposed controller, the part of control input that deals with uncertainty and disturbance is the switching term as given in equation (16) and (17) can be written as shown in equation (27) below

$$v_n = -k_2|\sigma_1|^{1/2}sign(\sigma_1) - k_3\int sign(\sigma_1)dt \tag{27}$$

where k_2 and k_3 are given as mentioned in [6] as:

$$k_3 > \frac{\zeta}{\Gamma_{min}} \tag{28}$$
$$(k_2)^2 > \frac{4\zeta\Gamma_{max}(k_3 + \zeta)}{\Gamma_{min}^2\Gamma_{min}(k_3 - \zeta)} \tag{29}$$

with conditions

$$\zeta > |\frac{d\dot{\sigma}_1}{dt} + \frac{\dot{\sigma}_1}{dz}[f(z,t) + b(t)v(t) + \delta_1(t)]| \tag{30}$$

and

$$0 \leq \Gamma_{min} \leq |\frac{d\dot{\sigma}_1}{dt}| \leq \Gamma_{max} \tag{31}$$

The requirements to meet for the system to be stable are: V is positive definite and radially unbounded, where as $\dot{V}$ is negative definite .
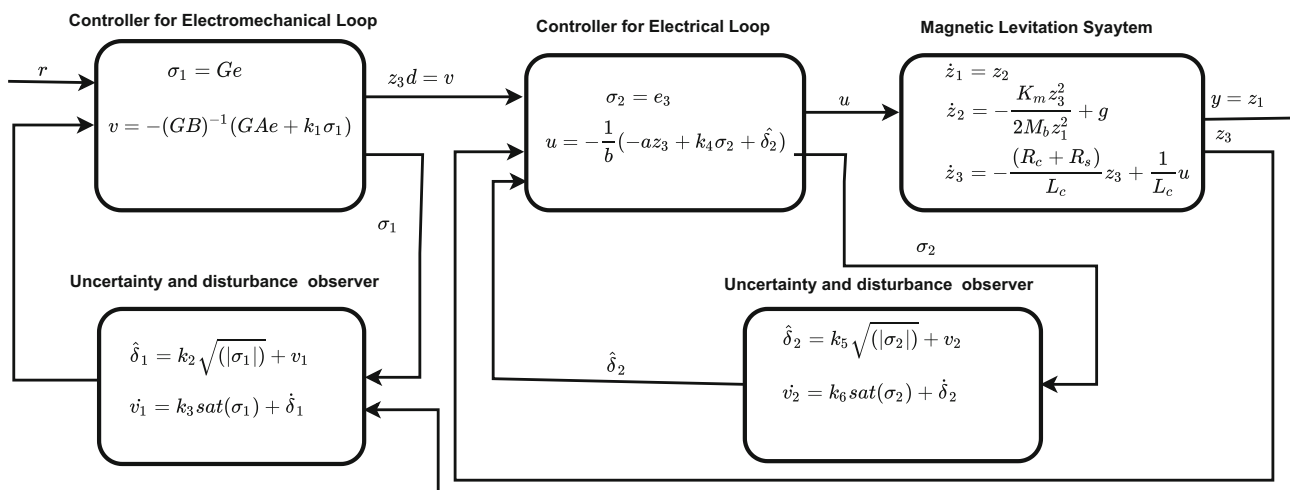
Fig. 2 Block diagram for proposed controller

Using the Lyapunov candidate function as follows:

$$V = \frac{1}{2}\sigma_1^2 \tag{32}$$

The first two requirements are met by Eq. (32), the time derivative of Eq. (32) is as follows:

$$\dot{V} = \sigma_1\dot{\sigma_1} \tag{33}$$

Substituting $\dot{\sigma_1}$ from Eq. (13) in Eq. (33)

$$\dot{V} = \sigma_1(GAe + GBv + GB\delta_1) \tag{34}$$

putting the value of v from section 3 in Eq.(34) and simplifying

$$\dot{V} = \sigma_1(-k_1\sigma_1 - k_2|\sigma_1|^{1/2}sign(\sigma_1)$$
$$- k_3 \int sign(\sigma_1)dt - GB\delta_1) \tag{35}$$

Further simplifying

$$\dot{V} = -k_1\sigma_1^2 - k_2|\sigma_1|^{1/2}|\sigma_1|$$
$$- k_3 \int |\sigma_1| \, dt - GB\sigma_1\delta_1 \tag{36}$$

Equation (36) demonstrates that $\dot{V}$ is negative definite, which implies that setting parameters (k_3 and k_2) in accordance with (28) and (29) will ensure the controller's asymptotic stability.

4 Simulation results

This section uses simulation to assess the efficacy of the proposed control strategy. The results of the proposed method

are compared to those of a PID and SDO controller. PID is referred to as "Approach I", SDO is referred to as "Approach II", and the suggested method is referred to as "Approach III". The nominal plant parameters that were used in the simulation are shown in Table 1. A simulation is done using MATLAB/Simulink on the Maglev system depicted in Fig. 1 to demonstrate the effectiveness of the proposed controller. The following are the initial conditions of system states :

$$x(0) = \begin{bmatrix} 0.014 & 0 & 0 \end{bmatrix}^T,$$

Approach-I: A PID controller with a feed forward (PID-FF)component is suggested by [42] for the maglave system control is applied and tested for the system. The electromechanical loop in maglave is controlled with PID plus FF control and Proportional Integral(PI) control is applied to the electrical loop. Both the PID and feed forward controller gains are determined by root locus selection of closed loop poles that match the performance requirements. In PID controller design, three independent gains are employed, resulting in two zeros and a pole at the origin, converting the system to a Type 1 system with zero steady-state error. Adjusting for gravitational bias is the goal of the feed forward control operation. When the PID controller adjusts for dynamic disturbances around the linear operating point, the feed forward control action reduces the changes in gravitational bias-induced force. The nonlinear mathematical model of the plant was built using fundamental physical concepts and around the equilibrium point, the nonlinear equation was linearized using Taylor's series. Simple mathematical gain equations to obtain the needed response have been established by combining the tuning philosophy of PID controllers with the notion of LQR theory. The testing findings showed that the proposed strategy was effective not only in stabilizing the ball but in tracking the various reference trajectories

Table 1 Maglev system nominal parameters

Parameter	Value	Units
M_b	0.068	kg
R_s	1	Ω
g	9.81	m/s^2
R_c	10	Ω
K_m	6.580×10^{-5}	Nm^2/A^2
L_c	413	mH
T_b	0.014	m

that were provided as input. With the controller settings, $Ki_b = 524$, $K_{pb} = 208$, $K_{vb} = 3$, and $K_{ff} = 153$, the ball will track the required reference trajectory. A PI controller is used in the current loop to keep the actual current z_3 at the intended current level z_{3d}. $kp = 219$ and $ki = 50,000$ are the PI controller settings.

Approach-II: Cascaded sliding mode control is used for magnetic levitation systems, as designed in [25]. A disturbance observer-based sliding mode controller is utilized for the electrical loop, while a state and disturbance observer (SDO)-based sliding mode controller is used for the electromechanical loop. The SDO is used to estimate both the state and the uncertainty at the same time. The controller proposed for electrical loop is explained in brief. The observer dynamics are defined as

$$\left.\begin{aligned} \dot{\hat{e}} &= A\hat{e} + Bv + B\hat{\delta}_1 + M(y - \hat{y}) \\ y &= Ce \end{aligned}\right\} \quad (37)$$

where A, B, and C are matrices as defined earlier. M is observer gain matrix. The sliding surface is defined as,

$$\sigma_3 = G_1\hat{e} \quad (38)$$

where $G_1 = \begin{bmatrix} c_1 & 1 \end{bmatrix}$ and c_1 is a positive constant. After differentiating (38) and using (37) gives,

$$\dot{\sigma}_3 = G_1 A\hat{e} + G_1 Bv + G_1 B\hat{\delta}_1 + G_1 M(y - \hat{y}) \quad (39)$$

Design v as,

$$v = -\frac{1}{G_1 B}(G_1 A\hat{e} + k_7\sigma_3 + k_8 sat(\sigma_3)) - \hat{\delta}_1 \quad (40)$$

where k_7 and k_8 are positive constants.

Disturbance observer-based control strategy is suggested to achieve the goal of making $z_3 = z_{3d}$. The sliding surface defined is:

$$\sigma_4 = e_3 \quad (41)$$
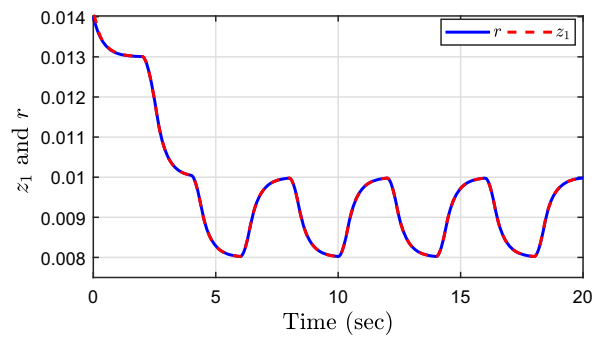
(a) Ball tracking for proposed controller
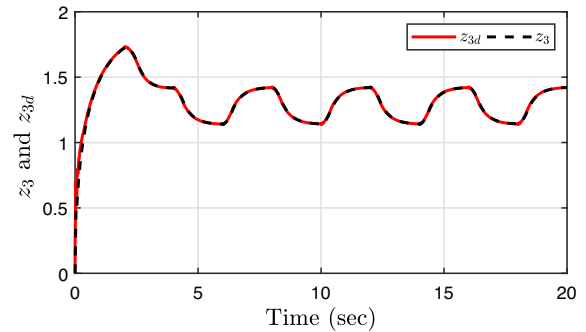
(b) Current input for proposed controller
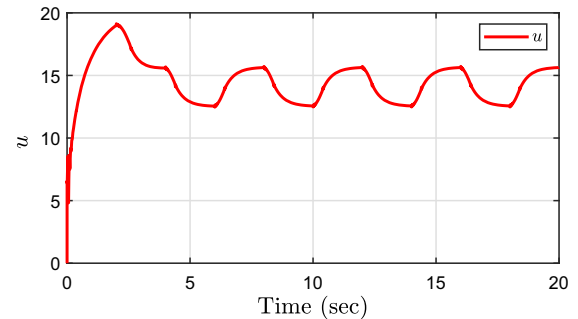
(c) Control input for proposed controller

Fig. 3 Simulation Results for proposed Controller with nominal plant
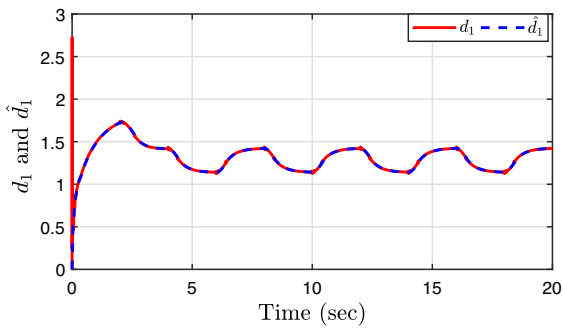
differentiating (41)

$$\dot{\sigma}_4 = -a_3 z_3 + bu + \delta_2 \quad (42)$$

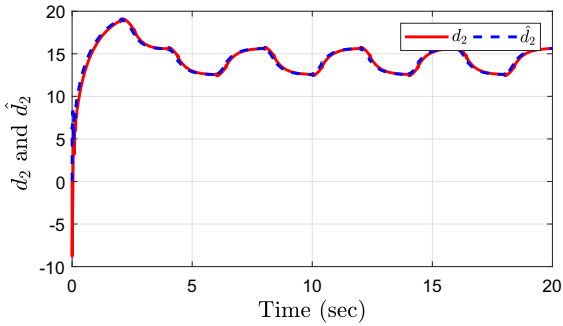Lets take $u = u_k + u_n$. Where u_k is designed to compensate for known terms as

$$u_k = -\frac{1}{b}(-a_3 z_3 + k_9\sigma_4 + k_{10} sat(\sigma_4)) \quad (43)$$

where the positive constants k_9 and k_{10} are used. Design

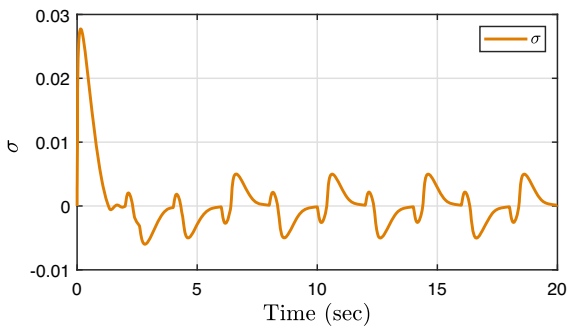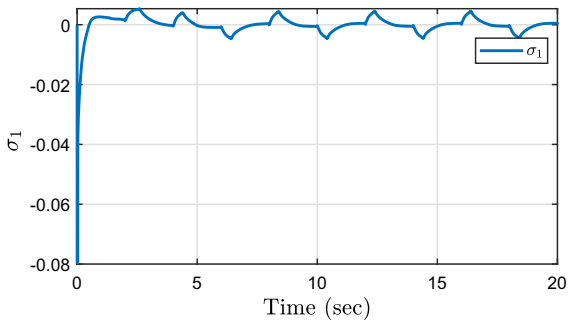$$u_n = -\frac{\hat{\delta}_2}{b} \quad (44)$$

(a) Disturbance and its estimation for electromechanical loop

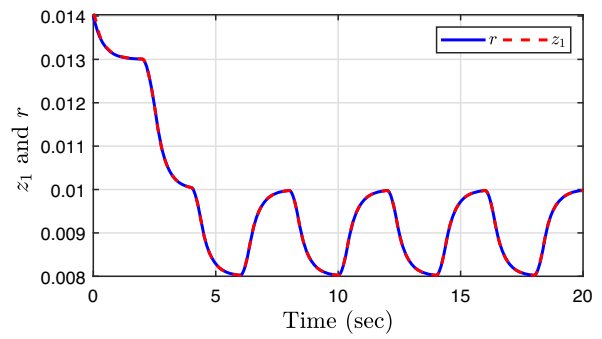**(b)** Disturbance and its estimation for electrical loop

(c) Sliding surface for electromechanical loop
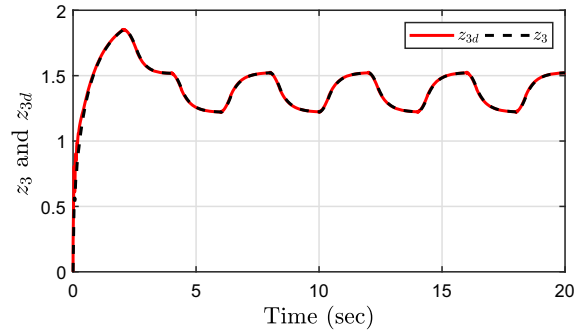

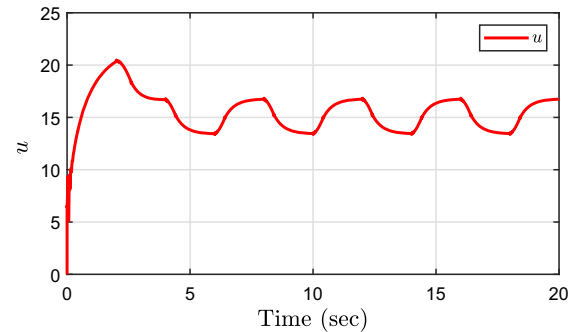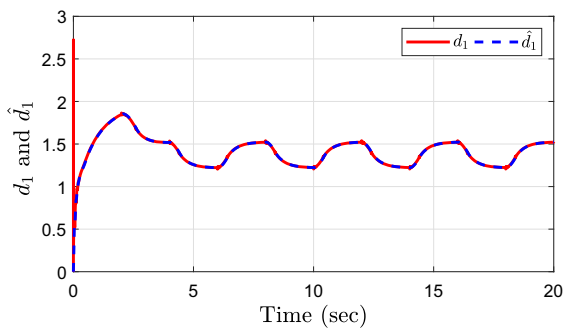**(d)** Sliding surface for electrical loop

Fig. 4 Simulation Results for proposed Controller with nominal plant

(a) Ball tracking for proposed controller

(b) Current input for proposed controller

(c) Control input for proposed controller

Fig. 5 Simulation Results for proposed Controller with 20% uncertainty in plant

where $\hat{\delta_2}$ is a estimate of δ_2, obtained using DO as

$$\hat{\delta}_2 = p + q_2\sigma_4 \tag{45}$$

where q_2 is user defined constant
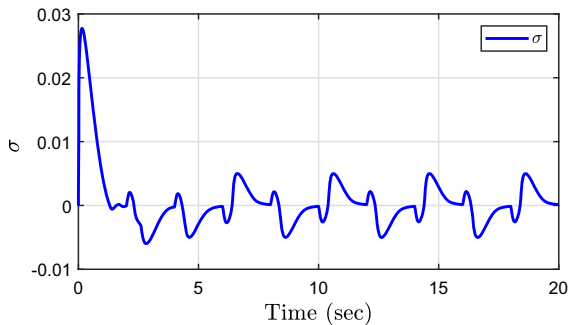
$$\dot{p} = -q_2\dot{\sigma}_4 \tag{46}$$

The controller parameters of SDO-based controller applied to the electromechanical subsystem and Do based controller for electrical subsystem are set as $k_7 = 35$, $k_8 = 35$, $k_9 = 3$, $\epsilon_3 = 0.05$ and $\epsilon_4 = 0.05$.
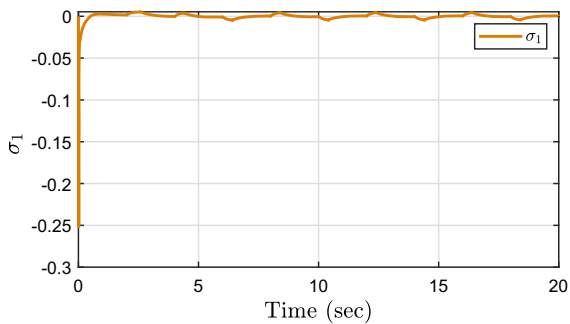
(a) Disturbance and its estimation for electromechanical loop
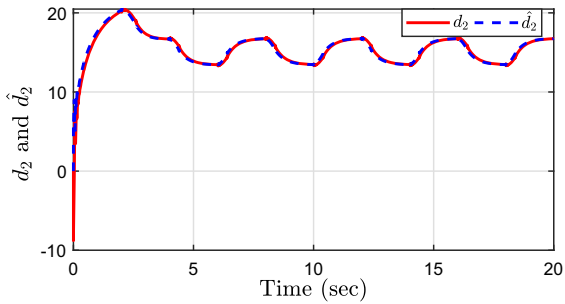
(b) Disturbance and its estimation for electrical loop
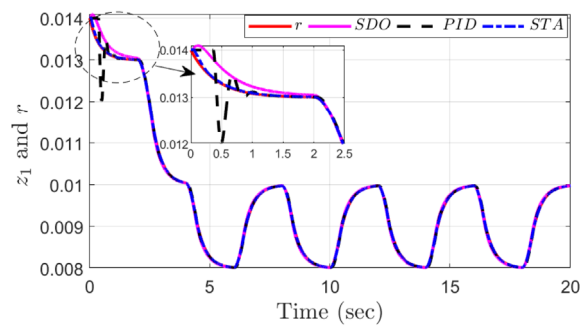

(c) Sliding surface for electromechanical loop
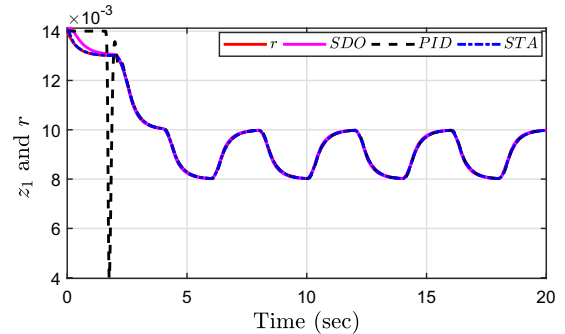

(d) Sliding surface for electrical loop

Fig. 6 Simulation Results for proposed Controller with 20% uncertainty in plant

(a) Ball tracking comparision for nominal plant

(b) Ball tracking comparision for plant with 20% uncertainty

Fig. 7 Comparison of simulation Results for proposed Controller with nominal plant and with uncertainty

Table 2 Performance comparison of controllers for nominal system

Controller	ISE	IAE	ITAE
STDO(proposed)	4.878×10^{-8}	0.000541	0.00390
SDO	1.268×10^{-7}	0.000915	0.00610
PID	2.313×10^{-7}	0.000623	0.00299

Table 3 Performance comparison of controllers for system with 20% uncertainty

| Controller	ISE	IAE	ITAE
STDO(proposed)	5.413×10^{-8}	0.000568	0.00399
SDO	1.48×10^{-7}	0.000981	0.00651
PID	9.436×10^{-6}	0.00287	0.00645

Approach-III: Proposed super twisting disturbance observer-based controller is referred as approach-III. The controller parameters for electromechanical loop are $k_1 = 25$, $k_2 = 10$, $k_3 = 0.01$, $\epsilon_1 = 0.05$ and for electrical loop are $k_4 = 50$, $k_5 = 2$, $k_6 = 45$, and $\epsilon_2 = 0.05$. The simulation results are shown in Fig. 3– 7. From Fig. 3a, it can be seen that the proposed controller makes the ball position, z_1 successfully track the reference r. The required current and the control input generated to make the ball position track the reference trajectory with proposed approach is shown in Fig. 3b,
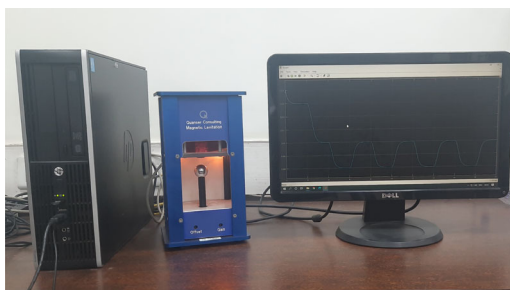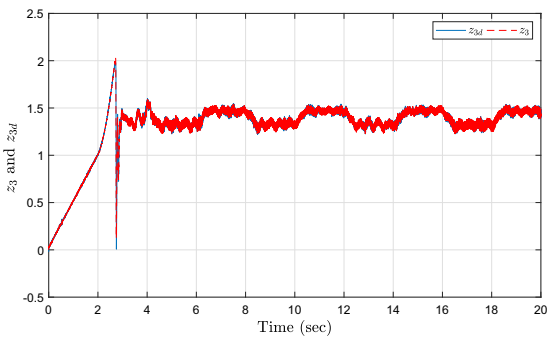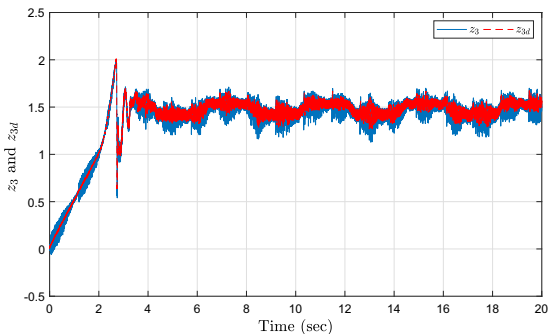
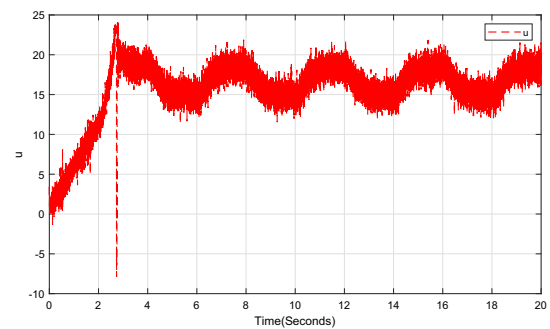(a) Magnetic levitation Setup (Quanser Inc.2010)

(b) Ball tracking for proposed controller
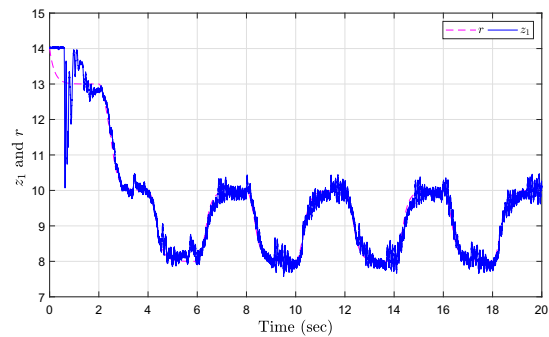
(c) Current input for proposed controller

(d) Control input for proposed controller

Fig. 8 Experimental Results for proposed Controller

(a) Ball tracking for SDO

(b) Current input forSDO

(c) Control input for SDO

Fig. 9 Experimental Results for SDO based controller

c respectively. The generated control input and current to achieve desired tracking performance are both within the maximum permitted limits. The designed super twisting estimator is able to estimate uncertainties d_1 and d_2 in two loops of the maglave. The plots of d_1 and d_2 with its respective estimate $\hat{d}_1$ and $\hat{d}_2$is given in Fig. 4a, b respectively. To compensate for the influence of uncertainties, the suggested control law employs the opposite of these estimations. Sliding surfaces used for the control of electromechanical and electrical loops are shown in Fig. 4c, d respectively.

The same plant is simulated by taking parametric uncertainty of 20% and the tracking performance along with control input, current, uncertainty estimation is shown in Figs. 5 and 6. The comparative tracking results for all three
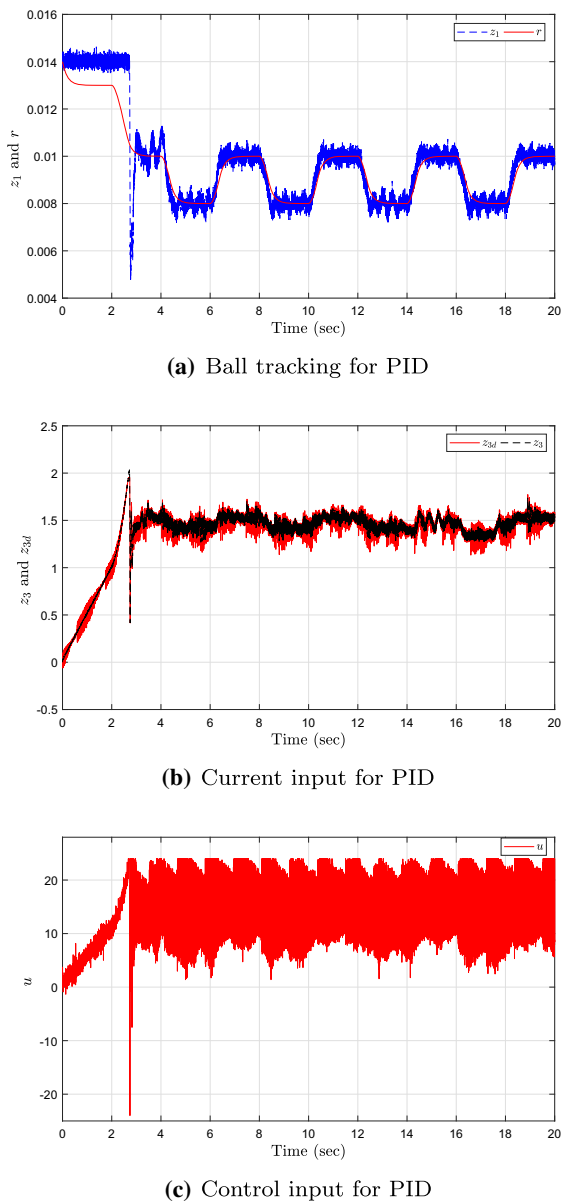
(a) Ball tracking for PID

(b) Current input for PID

(c) Control input for PID

Fig. 10 Experimental Results for PID controller

controllers are depicted in Fig. 7a, b for nominal and system with uncertainty. It clearly shows that proposed controller is performing better than the other two controllers.

5 Experimental Results

The proposed controller architecture is validated experimentally utilizing a magnetic levitation laboratory setup [43] shown in Fig. 8a. A solid one inch steel ball is suspended by an electromagnetic suspension mechanism in the Maglev system. It is basically made up of an electromagnet located towards the top of the apparatus, which is capable of lifting

the steel ball from its pedestal and sustaining it in free space. Two system variables are instantly monitored and offered for feedback on the configuration. The two variables are the coil current and the ball distance from the magnetic face. The ferromagnetic ball travels between 0 and 14 mm, however the linear range of the optical sensor used to detect ball location is between 6 and 14 mm . The range of the control input is between 0 to 24 V and the input current range is between 0 to 3 A . The controller parameters and initial conditions of Approach-I, II and III are set to the same values as in the simulation. The tracking performance, control input voltage and input current graphs are shown for all three controllers in Figs. 8, 9 and 10. The experimental validation indicates that the tracking performance of the proposed controller is better as compared to the other.

5.1 Comparison of proposed controller with PID and SDO

The efficacy of the suggested method is evaluated in this part using simulation and experimentation. The suggested scheme's results are compared to those of a linear PID controller and an SDO-based controller. The suggested controller's efficacy is tested for nominal systems and systems with 20% parametric uncertainty. The graphical depiction demonstrates that the suggested technique provides improved tracking by keeping control input within a given limits. The outcomes are assessed using error-based performance metrics such as IAE, ITAE, and ISE. Table 2 summaries the performances of all three types of controller on the basis of error-based criteria for system with nominal parameters. Table 3 shows performance comparison for all three controllers when applied for plant with 20% uncertainty. The results in the table clearly demonstrate that the proposed controller's performance is superior to the other two .

6 Conclusion

Cascaded super twisting disturbance observer-based SMC, SDO-based SMC and PID controllers are applied and discussed for tracking control of a magnetic levitation plant. The proposed control scheme is immune to uncertainties and the reference trajectory to be tracked, contrasting methods that depend on approximate linearization. The whole system's stability has been demonstrated. In simulation and experimental validation, the suggested approach outperforms conventional PID- and SDO-based controller. The performance of proposed controller is compared on the basis of error-based criteria with other two controllers and the comparison shows superiority of the proposed scheme over the others. The findings demonstrate that the suggested controller

can stabilize the magnetic levitation system from difficult start-up circumstances to the desired operating points with smooth control. It is capable of dealing with intrinsically unstable nonlinear dynamics and can deal with uncertain model with external noise as well.

Declarations

Conflicts of interest The authors have no conflicts of interest to declare that are relevant to the content of this article.

References

1. Goodall R, Kortüm W (1983) Active controls in ground transportation-a review of the state-of-the-art and future potential. Veh Syst Dyn 12(4–5):225–257
2. Rote D, Cai Y (2002) Review of dynamic stability of repulsive-force maglev suspension systems. IEEE Trans Magn 38(2):1383–1390
3. Givoni M (2006) Development and impact of the modern high-speed train: A review. Transp Rev 26(5):593–611
4. Lee H-W, Kim K-C, Lee J (2006) Review of maglev train technologies. IEEE Trans Magn 42(7):1917–1925
5. Eroğlu Y, Ablay G (2016) Cascade sliding mode-based robust tracking control of a magnetic levitation system. Proc Inst Mech Eng, Part I: J Syst Control Eng 230(8):851–860
6. Adil HMM, Ahmed S, Ahmad I (2020) Control of maglev system using supertwisting and integral backstepping sliding mode algorithm. IEEE Access 8:51352–51362
7. Matsumura F, Yoshimoto T (1986) System modeling and control design of a horizontal-shaft magnetic-bearing system. IEEE Trans Magn 22(3):196–203
8. Cho D, Kato Y, Spilman D (1993) Sliding mode and classical controllers in magnetic levitation systems. IEEE Control Syst Mag 13(1):42–48
9. Yeh T-J, Chung Y-J, Wu W-C (2001) Sliding control of magnetic bearing systems. J Dyn Sys Meas Control 123(3):353–362
10. Lin F-J, Teng L-T, Shieh P-H (2007) Intelligent sliding-mode control using rbfn for magnetic levitation system. IEEE Trans Industr Electron 54(3):1752–1762
11. Green SA, Craig KC (1998) Robust, digital, nonlinear control of magnetic-levitation systems. J Dyn Syst Meas Contr 120(4):488–495
12. Chen M-Y, Wu K-N, Fu L-C (2000) Design, implementation and self-tuning adaptive control of maglev guiding system. Mechatronics 10(1–2):215–237
13. Barie W, Chiasson J (1996) Linear and nonlinear state-space controllers for magnetic levitation. Int J Syst Sci 27(11):1153–1163
14. Yang Z-J, Miyazaki K, Kanae S, Wada K (2004) Robust position control of a magnetic levitation system via dynamic surface control technique. IEEE Trans Industr Electron 51(1):26–34
15. Lin F-J, Chen S-Y, Shyu K-K (2009) Robust dynamic sliding-mode control using adaptive renn for magnetic levitation system. IEEE Trans Neural Networks 20(6):938–951
16. Chen K-Y, Tung P-C, Tsai M-T, Fan Y-H (2009) A self-tuning fuzzy pid-type controller design for unbalance compensation in an active magnetic bearing. Expert Syst Appl 36(4):8560–8570
17. Baranowski J, Piatek P (2012) Observer-based feedback for the magnetic levitation system. Trans Inst Meas Control 34(4):422–435
18. Michail K, Zolotas A, Goodall R, Whidborne J (2012) Optimised configuration of sensors for fault tolerant control of an electromagnetic suspension system. Int J Syst Sci 43(10):1785–1804
19. Wai R-J, Lee J-D, Chuang K-L (2011) Real-time pid control strategy for maglev transportation system via particle swarm optimization. IEEE Trans Industr Electron 58(2):629–646
20. Lin C-M, Lin M-H, Chen C-W (2011) Sopc-based adaptive pid control system design for magnetic levitation system. IEEE Syst J 5(2):278–287
21. Morales R, Feliu V, Sira-Ramirez H (2011) Nonlinear control for magnetic levitation systems based on fast online algebraic identification of the input gain. IEEE Trans Control Syst Technol 19(4):757–771
22. Yang J, Zolotas A, Chen W-H, Michail K, Li S (2011) Robust control of nonlinear maglev suspension system with mismatched uncertainties via dobc approach. ISA Trans 50(3):389–396
23. Zhang Y, Xian B, Ma S (2015) Continuous robust tracking control for magnetic levitation system with unidirectional input constraint. IEEE Trans Industr Electron 62(9):5971–5980
24. Al-Araji AS (2016) Cognitive non-linear controller design for magnetic levitation system. Trans Inst Meas Control 38(2):215–222
25. Ginoya D, Gutte CM, Shendge P, Phadke S (2016) State-and-disturbance-observer-based sliding mode control of magnetic levitation systems. Trans Inst Meas Control 38(6):751–763
26. Mane H, Wanaskar V, Chaudhari S, Shendge PD, Phadke SB (2021) Novel two time scale observer based sliding mode control with velocity estimator for magnetic levitation. In: 2021 International Conference on Smart Generation Computing, Communication and Networking (SMART GENCON), pp. 1–6
27. Tepljakov A, Alagoz BB, Gonzalez E, Petlenkov E, Yeroglu C (2018) Model reference adaptive control scheme for retuning method-based fractional-order pid control with disturbance rejection applied to closed-loop control of a magnetic levitation system. J Circ, Syst Comput 27(11):1850176
28. Sadek U, Sarjaš A, Chowdhury A, Svečko R (2017) Improved adaptive fuzzy backstepping control of a magnetic levitation system based on symbiotic organism search. Appl Soft Comput 56:19–33
29. Bidikli B, Bayrak A (2018) A self-tuning robust full-state feedback control design for the magnetic levitation system. Control Eng Pract 78:175–185
30. Oh S-Y, Choi H-L (2018) Robust approximate feedback linearisation control for nonlinear systems with uncertain parameters and external disturbance: its application to an electromagnetic levitation system. Int J Syst Sci 49(12):2695–2703
31. Adıgüzel F, Dokumacılar E, Akbatı O, Türker T (2018) Design and implementation of an adaptive backstepping controller for a magnetic levitation system. Trans Inst Meas Control 40(8):2466–2475
32. Khimani D, Karnik S, Patil M (2018) IFAC-PapersOnLine. In: 5th IFAC Conference on Advances in Control and Optimization of Dynamical Systems ACODS 51(1): 13–18
33. Humaidi AJ, Badr HM, Hameed AH (2018) Pso-based active disturbance rejection control for position control of magnetic levitation system. In: 2018 5th International Conference on Control, Decision and Information Technologies (CoDIT), pp. 922–928

34. Sun Y, Xu J, Qiang H, Chen C, Lin G (2019) Adaptive sliding mode control of maglev system based on rbf neural network minimum parameter learning method. Measurement 141:217–226

35. Sun Y, Xu J, Qiang H, Lin G (2019) Adaptive neural-fuzzy robust position control scheme for maglev train systems with experimental verification. IEEE Trans Industr Electron 66(11):8589–8599

36. Chen C, Xu J, Ji W, Rong L, Lin G (2019) Sliding mode robust adaptive control of maglev vehicle's nonlinear suspension system based on flexible track: Design and experiment. IEEE Access 7:41874–41884

37. Nerkar S, Londhe P, Patre B (2022) Design of super twisting disturbance observer based control for autonomous underwater vehicle. Int J Dyn Control 10(1):306–322

38. Levant A (1993) Sliding order and sliding accuracy in sliding mode control. Int J Control 58(6):1247–1263

39. Utkin VI, Poznyak AS (2013) Adaptive sliding mode control with application to super-twist algorithm: equivalent control method. Automatica 49(1):39–47

40. Chalanga A, Kamal S, Fridman LM, Bandyopadhyay B, Moreno JA (2016) Implementation of super-twisting control: Super-twisting and higher order sliding-mode observer-based approaches. IEEE Trans Industr Electron 63(6):3677–3685

41. Yan R, Wu Z (2019) Super-twisting disturbance observer-based finite- time attitude stabilization of flexible spacecraft subject to complex disturbances. J Vib Control 25(5):1008–1018

42. Vinodh Kumar E, Jerome J (2013) Lqr based optimal tuning of pid controller for trajectory tracking of magnetic levitation system. Procedia Engineering, vol. 64, pp. 254–264. International Conference on Design and Manufacturing (IConDM2013)

43. Magnetic levitation plant user manual. Ontario, Canada: Qunaser Inc (2010)